ORIGINAL ARTICLE

Predictive value of gemstone spectral imaging for chemotherapy response in colorectal cancer liver metastases: A retrospective study

Hou-Fa Ning[1,2], Yun-Long Qin[3], Kui-Tao Yue[1,2], Shuai Wang[2,4], Wei-Guang Shao[1,2], Guang-Zhi Wang[1,2]

[1]Department of Medical Imaging Center, Affiliated Hospital of Shandong Second Medical University, Weifang, Shandong, China, [2]Department of Radiology, School of Medical Imaging, Shandong Second Medical University, Weifang, Shandong, China, [3]Chest Pain Center, Interventional Catheter Center, Qilu Hospital of Shandong University, Jinan, China, [4]Department of Radiotherapy, Affiliated Hospital of Shandong Second Medical University, Weifang, Shandong, China

Background: Accurate and timely assessment of tumor response after chemotherapy is crucial in clinical settings. The aim of this study was to explore the feasibility of Gemstone Spectral Imaging (GSI) for early assessment of chemotherapy responses in patients with colorectal cancer liver metastasis (CRCLM). **Materials and Methods:** From October 2012 to October 2018, 46 patients (28 males and 18 females) with CRCLM received GSI followed by chemotherapy were retrospectively reviewed. The patients were divided into a response group (n = 32) and a nonresponse group (n = 14) according to the tumor response to chemotherapy. The iodine concentration images and virtual monoenergetic images (VMIs) with an optimal contrast-to-noise ratio at the arterial phase (AP) and portal venous phase (PVP) were obtained by GSI viewer. The iodine concentration value and computed tomography (CT) value on VMIs and slope of spectral attenuation curves of all lesions were compared. A logistic regression analysis was used to determine the predictor of chemotherapy response. **Results:** The difference of extrahepatic metastasis (P = 0.001), CT value on 68 keV VMIs at the AP (P = 0.005) and PVP (P = 0.001), slope of CT value attenuation curves at the AP (P = 0.013) and PVP (P = 0.001), and iodine concentration value at PVP (P = 0.003) between the response and nonresponse groups were statistically significant. The CT value of the 68 keV VMIs (OR: 1.206; 95% confidence interval [CI]: 1.021–1.425, P = 0.027) and the iodine concentration value at PVP (OR: 1.952; 95% CI: 1.034–3.684, P = 0.039) were independent prognostic factors for predicting chemotherapy response. **Conclusion:** Baseline GSI may help predict the response to chemotherapy and provide a good tumor-response indicator through single-energy CT value of 68 keV at the PVP and iodine concentration.

Key words: Chemotherapy, colorectal cancer, liver metastasis, prognosis, tomography X-ray computed

How to cite this article: Ning HF, Qin YL, Yue KT, Wang S, Shao WG, Wang GZ. Predictive value of gemstone spectral imaging for chemotherapy response in colorectal cancer liver metastases: A retrospective study. J Res Med Sci 2024;29:76.

INTRODUCTION

The liver is the main target organ for metastasis of colorectal cancer (CRC).[1,2] About 50% of patients eventually lead to liver metastasis, and more than 60% die from liver metastasis.[3,4] Chemotherapy combined with radical resection has become the standard treatment for CRC liver metastasis (CRCLM).[5,6] For unresectable patients, neoadjuvant chemotherapy can also control tumor progression and improve quality of life.[7-9] However, not all patients can benefit from primary chemotherapy. Therefore, the early prediction

Access this article online

Quick Response Code:

Website: https://journals.lww.com/jrms

DOI: 10.4103/jrms.jrms_630_23

Address for correspondence: Dr. Wei-Guang Shao, Department of Medical Imaging Center, Affiliated Hospital of Shandong Second Medical University, Weifang, Shandong, China.
E-mail: weiguangshao2004@163.com
Dr. Guang-Zhi Wang, Department of Medical Imaging Center, Affiliated Hospital of Shandong Second Medical University, Weifang, Shandong, China.
E-mail: guangzhiwang2000@163.com
Dr. Shuai Wang, Department of Radiotherapy, Affiliated Hospital of Shandong Second Medical University, Weifang, Shandong, China.
E-mail: sdwftcmws@163.com
Submitted: 22-Sep-2023; **Revised:** 08-Aug-2024; **Accepted:** 06-Nov-2024; **Published:** 31-Dec-2024

of chemotherapy response is essential in the choice of suitable treatment.

Traditional computed tomography (CT) scans provide relatively few parameters and reflect limited information on tissue microstructure changes. Gemstone Spectral Imaging (GSI) is based on quickly switching between high and low dual-energy (80 and 140 kVp) and obtaining dual-energy CT imaging data.[10] Through the reconstruction of two groups of data, multiparameter imaging is realized, including virtual monoenergetic images (VMIs), energy spectrum curves, and other material density images. It is helpful for the location and qualitative and quantitative analysis of lesions.[11,12] In this retrospective study, we investigated the feasibility of baseline GSI in evaluating the response to chemotherapy in patients with CRCLM.

SUBJECTS AND METHODS

Study design and patients

This study was in accordance with the Helsinki Declaration and approved by the institutional review board, and a waiver of informed consent was granted. The patients with CRCLM who underwent GSI examinations followed by chemotherapy in the Affiliated Hospital of Shandong Second Medical University from October 2012 to October 2018 were included in this study. Inclusion criteria: (1) pathological or clinical confirmed CRCLM; (2) completed abdomen GSI examination; and (3) received chemotherapy as the first-line treatment after GSI examination no more than 2 weeks. Exclusion criteria: (1) previously received chemotherapy, molecular targeted therapy, or biological therapy and (2) received local treatment of liver tumors, including but not limited to surgery, interventional therapy, radiofrequency ablation, microwave ablation, and other treatments.

Computed tomography examination

A single-source 64-channel CT scanner with rapid kVp switching dual-energy technology (Discovery CT750, GE Healthcare, Wisconsin, USA) was used for CT examination. Unenhanced scanning was performed in the conventional helical mode. A total of 90–120 mL (1.5 mL/kg) nonionic contrast medium (Omnipaque, GE Healthcare, 300 mg/ml) was administered for contrast enhancement scanning at an injection rate of 3–4 mL/s followed by 40 mL saline solution. The arterial phase was acquired at 30 s and the venous phase 55 s after bolus triggering with abdominal GSI scanning mode: dual kV/Adaptive mA technology, rotation time of 0.8 s, slice thickness of 5 mm, interval of 5 mm, collimation of 64 mm × 0.625 mm, and helical pitch of 1.375:1.

Image postprocessing and analysis

An adaptive statistical iterative reconstruction algorithm (ASiR, GE Healthcare, Milwaukee, WI, USA) was applied, and all images were transferred to Workstation 4.6 (GE Advantage Workstation 4.6, GE Medical Systems). Using the GSI viewer software, the mixed-energy images, mono-energy images at arterial phase and portal venous phase, and iodine concentration images were automatically obtained. Two radiologists (each with 10 years of radiology experience) observed and analyzed all the images and placed a region of interest on the images (avoiding bleeding, necrosis, and cystic portions) where the maximum diameter of the tumor was located.[13] The best contrast-to-noise ratio (CNR) monoenergetic images and iodine concentration images were selected for analysis. The spectral curves of the metastases in the arterial and portal venous phases were depicted with an interval of 10 keV, and two points of 50 keV (CT50) and 100 keV (CT100) were selected as reference points on the energy spectrum curve and measured CT values. To calculate the curve slopes (k), the following equation was used: $\kappa = CT50 - T100/(100 - 50keV)$.

Response evaluation

Mixed-energy images before chemotherapy were used as the baseline for tumor evaluation. The response was evaluated by routine CT or magnetic resonance imaging every 6–8 weeks after chemotherapy. Tumor response was determined according to the response evaluation criteria in solid tumors (RECIST 1.1).[14] Tumor response included: (1) complete response (CR): complete disappearance of all target lesions; (2) particle response (PR): compared with the baseline, the sum of the largest focus diameter decreased by more than 30%; (3) progress of disease (PD): the sum of the largest diameter lesions increased by more than 20%; and (4) stability of disease (SD): between PR and PD. Patients with CR or PR were classified into response group, whereas patients with SD or PD were classified into nonresponse group.[15]

Statistical analysis

All continuous variables were expressed as mean ± standard deviation (SD) or as medians, and categorical data were presented as frequencies and percentages. The interobserver consistency of two radiologists was assessed by interclass correlation coefficient (ICC), whereas paired t-test was used for difference analysis. A t-test or Mann–Whitney U-test was used to compare the parameters between the chemotherapy response group and the nonresponse group. Univariate and multiple logistic regression analyses were used to determine the independent predictors of chemotherapy response. The variates with statistical differences corresponding to chemotherapy were determined by univariate regression analysis and then entered multiple logistic regression model. To evaluate the efficiencies of risk factors determined by multiple regression for predicting chemotherapy response, receiver operating characteristic (ROC) analyses were used. All statistical analyses were performed using

statistics software (SPSS, version 26.0, IBM, USA). $P < 0.05$ was considered statistically significant.

RESULTS

Gemstone Spectral Imaging features of colorectal cancer liver metastasis

A total of 46 patients (28 males and 18 females, 60.0 ± 10.0 years) who received chemotherapy as the first-line treatment within half a month after the GSI examination were included [Table 1].

There were 32 patients in the chemotherapy response group and 14 patients in the nonresponse group. The median energy level corresponding to the best CNR at the arterial phase and portal venous phase was 68 keV [Figure 1]. Therefore, the monoenergetic images at 68 keV were used for image analysis. The values of all parameters measured by two radiologists were assessed by ICCs, which showed no significant difference and excellent repeatability [Table 2]. The mean values measured by the two observers were used for subsequent analysis. The iodine concentration of hepatic metastases at the arterial and portal venous phases was significantly different (0.615 ± 0.350 mg/ml vs. 1.368 ± 0.532 mg/ml, $P < 0.001$). The slopes of Hounsfield unit attenuation curves of lesions at the arterial and portal venous phases were significantly different [0.477 ± 0.267 vs. 0.753 ± 0.391, $P < 0.001$, Figure 2a].

Difference analysis and predictive value analysis of the Gemstone Spectral Imaging

The iodine concentrations at the arterial phase in the response and nonresponse group were 0.510 ± 0.351 mg/ml and 0.661 ± 0.345 mg/ml ($P = 0.179$). The slopes of HU attenuation curves of lesions at the arterial and portal venous phases between the response and nonresponse groups showed statistically significance [$P = 0.006$ and $P < 0.001$, respectively, Figure 2b]. Univariate logistic regression analysis showed that extrahepatic metastasis ($P = 0.001$); CT value of 68 keV VMIs ($P = 0.005$) and slope of energy spectrum curve ($P = 0.013$) in the arterial phase; CT value of 68keV VMIs ($P = 0.001$) and slope of energy spectrum curve ($P = 0.001$); and iodine concentration ($P = 0.003$) in the portal vein phase were the influencing factors of chemotherapy response. Multivariate logistic regression analysis showed that the CT values of 68 keV VMIs ($P = 0.027$,

Table 1: Baseline characteristics of 46 patients

	Overall (*n*=46), *n* (%)	Nonresponse (*n*=14), *n* (%)	Response (*n*=32), *n* (%)	*P**
Age, mean±SD	59.96±10.02	60.93±10.25	59.53±10.05	0.668**
Gender (%)				
Male	28 (60.9)	6 (42.9)	22 (68.8)	0.184
Female	18 (39.1)	8 (57.1)	10 (31.2)	
ECOG PS				
PS 0	19 (41.3)	6 (42.9)	13 (40.6)	1
PS 1	27 (58.7)	8 (57.1)	19 (59.4)	
Child-Pugh				
A	34 (73.9)	10 (71.4)	24 (75.0)	1
B	12 (26.1)	4 (28.6)	8 (25.0)	
Primary tumor				
Colon	30 (65.2)	10 (71.4)	20 (62.5)	0.804
Rectum	16 (34.8)	4 (28.6)	12 (37.5)	
Primary tumor resection				
No	26 (56.5)	8 (57.1)	18 (56.2)	1
Yes	20 (43.5)	6 (42.9)	14 (43.8)	
CEA level (ng/mL)				
≤30	33 (71.7)	11 (78.6)	22 (68.8)	0.745
>30	13 (28.3)	3 (21.4)	10 (31.2)	
Multiple				
Multiple	32 (69.6)	14 (100.0)	18 (56.2)	0.009
Solitary	14 (30.4)	0	14 (43.8)	
Type				
Synchronous	25 (54.3)	7 (50.0)	18 (56.2)	0.944
Metachronous	21 (45.7)	7 (50.0)	14 (43.8)	
Extra hepatic metastases (%)				
Negative	16 (34.8)	10 (71.4)	6 (18.8)	0.002
Positive	30 (65.2)	4 (28.6)	26 (81.2)	

*Chi-squared test for categorical variate; **t-test for continuous variates. ECOG=Eastern Cooperative Oncology Group; PS=performance status; CEA=Carcinoembryonic antigen; SD=Standard deviation

OR: 1.206; 95% confidence interval [CI]: 1.021–1.425) and iodine concentration (P = 0.039, OR: 1.952; 95% CI: 1.034–3.684) in the portal vein phase were independent predictors [Table 3].

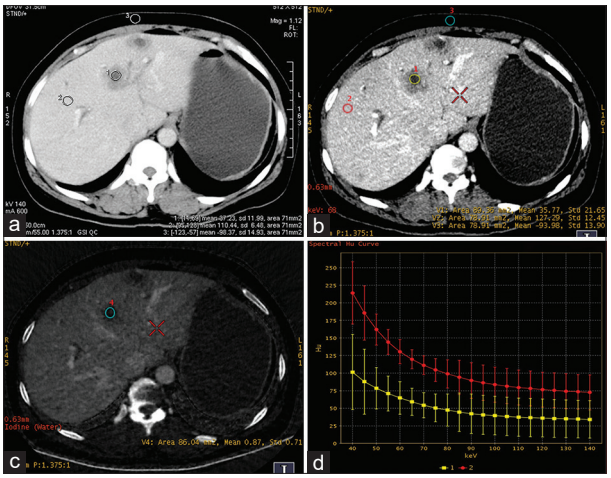

Figure 1: Gemstone spectral images of a patient with multiple hepatic metastases from colorectal cancer (portal venous phase). Female, age 35 years. (a) Mixed-energy image mark 1 is liver metastases (37.23 HU); (b) monoenergetic (68 keV) image shows that the edge of the lesion is clear (89.36 HU); (c) The iodine concentration of the lesions is 0.87; (d) The HU attenuation curve illustrates that the metastases (curve 1) have lower attenuation than the liver parenchyma (curve 2)

In ROC curve analyses [Figure 2c], the area under the curve of CT values of 68 keV VMIs and iodine concentration in the portal vein phase for predicting chemotherapy response was 0.949 (95% CI: 0.840–0.992) and 0.938 (95% CI: 0.825–0.988), and the difference between CT values and iodine concentration showed no statistically significant (P = 0.802). The cutoff values, sensitivity, specificity of CT values, and iodine concentration were 48.43 Hu, 93.75%, 92.86%, and 1.30 mg/ml, 75.0%, 100%, respectively. In addition, the Youden index of CT values and iodine concentration were 0.8661 and 0.750.

DISCUSSION

Our study shows that baseline spectral CT scans could help predict the efficacy of chemotherapy. Spectral CT is less vulnerable to artifacts such as beam hardening and pseudoenhancement, obtains absolute CT values of tissues under different single energy, and reflects the characteristics of tissues.[16] GSI can obtain CT values of substances with different energy levels (from 40 to 140 keV) and iodine concentration, which provide more reliable information than conventional CT images.[17,18] In our study, the median energy level corresponding to the best CNR in the arterial and portal phases was 68 keV, and it was found that the

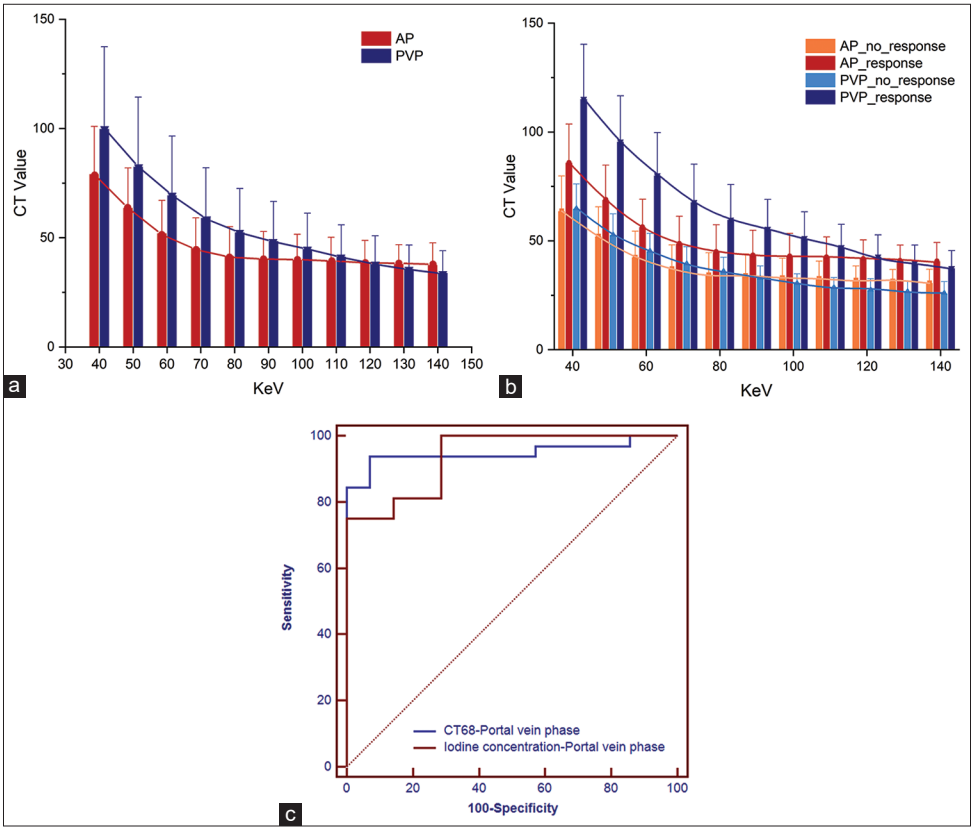

Figure 2: The characteristic of lesions on virtual monoenergetic images at the arterial and portal venous phases. (a) The slope of the HU attenuation curve of liver metastases at the portal venous phase was higher than that at the arterial phase (P < 0.001). (b) The slope of the HU attenuation curve of liver metastases at arterial phase and portal vein phase chemotherapy response groups were higher than that in nonresponse group (P = 0.006 and P < 0.001, respectively). (c) Receiver operating characteristic curves of CT values at 68 keV and iodine concentration in the portal vein phase for predicting chemotherapy response

Table 2: Evaluation of interrater variability and reproducibility of computed tomography values, spectral curves, and iodine concentration of single-energy images in arterial and portal venous phases

Parameter	Observer 1, mean±SD	Observer 2, mean±SD	*t*	*P**	ICC (95% CI)	*P***
AP						
CT-68keV (HU)	46.69±12.11	45.33±12.20	0.999	0.323	0.976 (0.957–0.987)	<0.001
k	0.47±0.17	0.48±0.15	0.837	0.407	0.944 (0.900–0.968)	<0.001
Iodine concentration (mgI/mL)	0.61±0.36	0.62±0.35	0.178	0.859	0.985 (0.972–0.991)	<0.001
PVP						
CT-68keV (HU)	58.27±16.34	58.38±15.92	0.335	0.739	0.991 (0.983–0.995)	<0.001
k	0.75±0.28	0.75±0.28	0.370	0.714	0.958 (0.926–0.977)	<0.001
Iodine concentration (mgI/mL)	1.36±0.53	1.37±0.53	0.628	0.533	0.984 (0.972–0.991)	<0.001

*Paired *t*-test for difference analysis; ***F*-test with true value 0 for ICC. ICC=Interclass correlation coefficient; CI=Confidence interval; SD=Standard deviation; AP=Arterial phase; PVP=Portal venous phase

Table 3: Univariate and multivariate analysis of predictors of chemotherapy response to colorectal cancer liver metastasis

Factors	Univariate analysis, OR (95% CI)	*P**	Multivariate analysis, OR (95% CI)	*P***
Age	0.986 (0.925–1.051)	0.660		
Gender	2.933 (0.803–10.719)	0.104		
ECOG	1.096 (0.307–3.911)	0.888		
Primary tumor	1.500 (0.384–5.860)	0.560		
Child-Pugh	0.833 (0.204–3.409)	0.800		
Primary tumor resection	1.037 (0.292–3.686)	0.955		
CEA level	1.667 (0.380–7.317)	0.499		
Multiple	0	0.998		
Type	0.778 (0.221–2.740)	0.696		
Extra hepatic metastases	10.833 (2.515–46.662)	0.001		
CT 68 A	1.117 (1.033–1.208)	0.005		
CT 68 V	1.230 (1.088–1.391)	0.001	1.206 (1.021–1.425)	0.027
k A	777.188 (4.033–149,751.741)	0.013		
IC A	3.765 (0.546–25.974)	0.179		
k V	28,966,711.88 (739.167–1.135)	0.001		
IC V	3020.763 (15.985–570,840.621)	0.003	1.952 (1.034–3.684)	0.039

*Univariate logistic regression; **Multiple logistic regression analysis. ECOG=Eastern Cooperative Oncology Group; k A=Slope of energy spectrum curve in the arterial phase; IC A=Iodine concentration in the arterial phase; k V=Slope of energy spectrum curve in the portal venous phase; IC V=Iodine concentration in the portal venous phase; CEA=Carcinoembryonic antigen; OR=Odds ratio; CI=Confidence interval

CT value of the 68 keV VMIs was also an independent predictor of chemotherapy response. This is consistent with the results of previous studies that selected the best CNR.[19] Although the best CNR varied from individuals, previous studies showed that the optimal CNR in soft tissue was always located at the 50–70 keV, and the HU values and visual effects of VMIs at 70 keV are similar to 120 kVp conventional CT images.[19-21]

Iodine concentration from spectral CT reflects tumor-derived angiogenesis, which may be useful for predicting early recurrence of hepatocellular carcinoma (HCC).[22,23] In our study, there was no significant difference in the iodine concentration at the arterial phase between the response and the nonresponse group. However, there were significant differences in the iodine concentration in venous phase between the two groups. This may be explained by the fact that CRCLM has gradual contrast material accumulation and that CT image acquisitions in the venous phase would result in a higher iodine concentration than acquisitions in the arterial phase. In this regard, the venous phase may better reflect the blood supply in tumor than the arterial phase. In addition, by multivariate analysis, we found that iodine concentration in the portal venous phase was an independent predictor of chemotherapy response. In addition, Lee *et al*.[24] reported that the iodine map was more helpful than the linearly blended images in detecting residual tumors and providing more basis for the formulation of treatment strategies.[21,25] The spectral attenuation curve can accurately reflect tissue characteristics, which have potential value for determining the nature, tissue source, and prognosis of lesions.[26] With an increasing of keV, the energy spectrum decay of the lesions in the portal venous phase was higher than that in the arterial phase. There were significant differences in the slope of the spectral curve in the arterial phase and venous phase between the two groups, which may be related to the heterogeneity of the tumor.[27] Therefore, the slope of the spectral curve can improve the sensitivity of distinguishing liver tumors.

The role of spectral CT in distinguishing benign from malignant lesions and for assessment of therapeutic response has been evaluated in the abdomen.[16,28] Studies have shown that spectral CT imaging technology is an objective tool for predicting tumor response after chemoembolization of HCC,[29] which is similar to our study. Recent studies also have shown that spectral CT has made achievements in deep learning, especially in solving the problem of severe noise at low keV.[30] Differing from conventional CT, GSI can analyze the similarity of spectral characteristics between lesions before and after treatment, thereby analyzing the nature and origin of lesions, and realizing the transition from morphological imaging to functional imaging.

Our research has some limitations. First, this study is a retrospective analysis, and there may be unavoidable selection bias. Second, this was a single-center study that included relatively few cases. Furthermore, not all time points after chemotherapy were considered in this study. Therefore, further verified studies in a larger sample from multiple centers are needed. In the future, we will monitor the changes in various parameters after each chemotherapy cycle to further obtain more useful information to evaluate the chemotherapy response of liver metastases.

CONCLUSION

Our study provides a noninvasive and useful tool for predicting efficacy in patients with CRCLM. The single-energy CT value of 68 keV in the portal vein phase and iodine concentration may help predict the response to chemotherapy.

Financial support and sponsorship

This work was supported by grants from Shandong Province Medicine and Health Science and Technology Development Project (No. 2019WS596, 2019WS602) and Weifang Science and Technology Development Project (2022YX050, 2023YX053), Weifang Young Medical Talents Support Project (2024113), Scientific Research Development Fund of Affiliated Hospitals (Teaching Hospitals) of Shandong Second Medical University in 2024 (2024FYZ003).

Conflicts of interest

The authors declare that the research was conducted in the absence of any commercial or financial relationships that could be construed as a potential conflict of interest.

REFERENCES

1. Dekker E, Tanis PJ, Vleugels JL, Kasi PM, Wallace MB. Colorectal cancer. Lancet 2019;394:1467-80.
2. Siegel RL, Wagle NS, Cercek A, Smith RA, Jemal A. Colorectal cancer statistics, 2023. CA Cancer J Clin 2023;73:233-54.
3. O'Connor OJ, McDermott S, Slattery J, Sahani D, Blake MA. The use of PET-CT in the assessment of patients with colorectal carcinoma. Int J Surg Oncol 2011;2011:846512.
4. Ren L, Zhu D, Gu J, Jia B, Li J, Qin X, *et al*. Chinese guidelines for the diagnosis and comprehensive treatment of colorectal liver metastases (V. 2023). Clin Surg Oncol 2023;2:100013.
5. National Health Commission of the People's Republic of China. Chinese protocol of diagnosis and treatment of colorectal cancer (2020 edition). Zhonghua Wai Ke Za Zhi 2020;58:561-85.
6. Bhudia J, Glynne-Jones R, Smith T, Hall M. Neoadjuvant chemotherapy without radiation in colorectal cancer. Clin Colon Rectal Surg 2020;33:287-97.
7. Folprecht G, Grothey A, Alberts S, Raab HR, Köhne CH. Neoadjuvant treatment of unresectable colorectal liver metastases: Correlation between tumour response and resection rates. Ann Oncol 2005;16:1311-9.
8. Folprecht G, Gruenberger T, Bechstein WO, Raab HR, Lordick F, Hartmann JT, *et al.* Tumour response and secondary resectability of colorectal liver metastases following neoadjuvant chemotherapy with cetuximab: The CELIM randomised phase 2 trial. Lancet Oncol 2010;11:38-47.
9. Pietrantonio F, Mazzaferro V, Miceli R, Cotsoglou C, Melotti F, Fanetti G, *et al*. Pathological response after neoadjuvant bevacizumab- or cetuximab-based chemotherapy in resected colorectal cancer liver metastases. Med Oncol 2015;32:182.
10. Adam SZ, Rabinowich A, Kessner R, Blachar A. Spectral CT of the abdomen: Where are we now? Insights Imaging 2021;12:138.
11. Al-Najami I, Drue HC, Steele R, Baatrup G. Dual energy CT – A possible new method to assess regression of rectal cancers after neoadjuvant treatment. J Surg Oncol 2017;116:984-8.
12. Lv P, Lin XZ, Chen K, Gao J. Spectral CT in patients with small HCC: Investigation of image quality and diagnostic accuracy. Eur Radiol 2012;22:2117-24.
13. Wu J, Lv Y, Wang N, Zhao Y, Zhang P, Liu Y, *et al.* The value of single-source dual-energy CT imaging for discriminating microsatellite instability from microsatellite stability human colorectal cancer. Eur Radiol 2019;29:3782-90.
14. Eisenhauer EA, Therasse P, Bogaerts J, Schwartz LH, Sargent D, Ford R, *et al*. New response evaluation criteria in solid tumours: Revised RECIST guideline (version 1.1). Eur J Cancer 2009;45:228-47.
15. Zhou Y, Zhang HX, Zhang XS, Sun YF, He KB, Sang XQ, *et al.* Non-mono-exponential diffusion models for assessing early response of liver metastases to chemotherapy in colorectal Cancer. Cancer Imaging 2019;19:39.
16. Silva AC, Morse BG, Hara AK, Paden RG, Hongo N, Pavlicek W. Dual-energy (spectral) CT: Applications in abdominal imaging. Radiographics 2011;31:1031-46.
17. Agrawal MD, Pinho DF, Kulkarni NM, Hahn PF, Guimaraes AR, Sahani DV. Oncologic applications of dual-energy CT in the abdomen. Radiographics 2014;34:589-612.
18. Yu L, Leng S, McCollough CH. Dual-energy CT-based monochromatic imaging. Am J Roentgenol 2012;199:S9-15.
19. Reimer RP, Große Hokamp N, Fehrmann Efferoth A, Krauskopf A, Zopfs D, Kröger JR, *et al.* Virtual monoenergetic images from spectral detector computed tomography facilitate washout assessment in arterially hyper-enhancing liver lesions. Eur Radiol 2021;31:3468-77.
20. Rajiah P, Parakh A, Kay F, Baruah D, Kambadakone AR, Leng S. Update on multienergy CT: Physics, principles, and applications. Radiographics 2020;40:1284-308.
21. McCollough CH, Boedeker K, Cody D, Duan X, Flohr T, Halliburton SS, *et al.* Principles and applications of multienergy CT: Report of AAPM task group 291. Med Phys 2020;47:e881-912.
22. Luo N, Li W, Xie J, Fu D, Liu L, Huang X, *et al.* Preoperative normalized iodine concentration derived from spectral CT is

correlated with early recurrence of hepatocellular carcinoma after curative resection. Eur Radiol 2021;31:1872-82.
23. Wang J, Shen JL. Spectral CT in evaluating the therapeutic effect of transarterial chemoembolization for hepatocellular carcinoma: A retrospective study. Medicine (Baltimore) 2017;96:e9236.
24. Lee SH, Lee JM, Kim KW, Klotz E, Kim SH, Lee JY, *et al.* Dual-energy computed tomography to assess tumor response to hepatic radiofrequency ablation: Potential diagnostic value of virtual noncontrast images and iodine maps. Invest Radiol 2011;46:77-84.
25. Xiao JM, Hippe DS, Zecevic M, Zamora DA, Cai LM, Toia GV, *et al.* Virtual unenhanced dual-energy CT images obtained with a multimaterial decomposition algorithm: Diagnostic value for renal mass and urinary stone evaluation. Radiology 2021;298:611-9.
26. Gong HX, Zhang KB, Wu LM, Baigorri BF, Yin Y, Geng XC, *et al.* Dual energy spectral CT imaging for colorectal cancer grading: A preliminary study. PLoS One 2016;11:e0147756.
27. Auer TA, Feldhaus FW, Büttner L, Jonczyk M, Fehrenbach U, Geisel D, *et al.* Spectral CT hybrid images in the diagnostic evaluation of hypervascular abdominal tumors-potential advantages in clinical routine. Diagnostics (Basel) 2021;11:1539.
28. Parakh A, Patino M, Muenzel D, Kambadakone A, Sahani DV. Role of rapid kV-switching dual-energy CT in assessment of post-surgical local recurrence of pancreatic adenocarcinoma. Abdom Radiol (NY) 2018;43:497-504.
29. Choi WS, Chang W, Lee M, Hur S, Kim HC, Jae HJ, *et al.* Spectral CT-based iodized oil quantification to predict tumor response following chemoembolization of hepatocellular carcinoma. J Vasc Interv Radiol 2021;32:16-22.
30. Jensen CT, Wong VK, Wagner-Bartak NA, Liu X, Padmanabhan Nair Sobha R, Sun J, *et al.* Accuracy of liver metastasis detection and characterization: Dual-energy CT versus single-energy CT with deep learning reconstruction. Eur J Radiol 2023;168:111121.